

UC Davis

UC Davis Previously Published Works

Title

Second Guessing in Perceptual Decision-Making

Permalink

<https://escholarship.org/uc/item/6d04c1hc>

Journal

Journal of Neuroscience, 40(26)

ISSN

0270-6474

Authors

McLean, Charlotte S

Ouyang, Bowen

Ditterich, Jochen

Publication Date

2020-06-24

DOI

10.1523/jneurosci.2787-19.2020

Peer reviewed

1 Title: **Second guessing in perceptual decision-making**

2 Abbreviated title: Second guessing in perceptual decision-making

3 Authors: **Charlotte S. McLean^{1,2}, Bowen Ouyang^{1,2} and Jochen Ditterich^{1,3}**

4 ¹Center for Neuroscience and Dept. of Neurobiology, Physiology & Behavior,
5 University of California, Davis, Davis, CA 95618

6 ²These authors have contributed equally to this work.

7 ³Corresponding author: jditterich@ucdavis.edu

8 Number of pages: 44

9 Number of figures: 8

10 Number of tables: 2

11 Number of multimedia: 0

12 Number of 3D models: 0

13 Number of words in abstract: 138

14 Number of words in introduction: 623

15 Number of words in discussion: 1,499

16 Conflict of interest statement: The authors declare no competing financial interests.

17 Acknowledgments: This study was supported by NSF grant 1156601.

18 Charlotte McLean is currently affiliated with the University of
19 Texas Southwestern Medical Center.

20

21 **ABSTRACT**

22 Human subjects of both sexes were asked to make a perceptual decision between multiple directions of
23 visual motion. In addition to reporting a primary choice, they also had to report a second guess,
24 indicating which of the remaining options they would rather bet on, assuming that they got their
25 primary choice wrong. The second guess was clearly informed by the amounts of sensory evidence that
26 were provided for the different options. A single computational integration-to-threshold model, based
27 on the assumption that the second guess is determined by the rank ordering of accumulated evidence at
28 or shortly after the time of the decision, was able to explain the distribution of primary choices,
29 associated response times, and the distribution of second guesses. This suggests that the decisionmaker
30 has access to how well supported unchosen options are by the sensory evidence.

31

32 **SIGNIFICANCE STATEMENT**

33 Perceptual decisions require conversion of sensory evidence into a discrete choice. Computational
34 models based on the accumulation of evidence to a decision threshold can explain the distribution of
35 choices and associated decision times. Subjects are also able to report the level of confidence in their
36 decision. Here we show that, when making decisions between more than two alternatives, the
37 decisionmaker can even report a second guess that is clearly informed by the sensory evidence. These
38 second guesses show a distribution that is consistent with subjects having access to how much sensory
39 evidence was accumulated for the unchosen options. The decisionmaker therefore has knowledge about
40 the outcome of the decision process that goes beyond just the choice and an associated confidence.

41

42

43 INTRODUCTION

44 Perceptual decisions require a decisionmaker to make a discrete choice on the basis of sensory
45 information. Substantial work has gone into elucidating the mechanisms that allow the inflowing
46 sensory evidence to be converted into a discrete choice. Integration-to-threshold mechanisms are the
47 currently dominant class of models, the Drift Diffusion Model (DDM) being a popular exemplar (Luce,
48 1986; Ditterich, 2006; Ratcliff and McKoon, 2008; Ditterich, 2010; Forstmann et al., 2016). These models
49 are based on the idea that sensory evidence for each available option is accumulated until the
50 accumulated evidence for one of the options exceeds a decision threshold. They can explain the
51 distribution of choices and associated response times (RTs) for a wide range of decision tasks (Ratcliff
52 and Smith, 2004) and are consistent with decision-related neural activity, both averaged across trials as
53 well as on a single-trial level (Ditterich, 2006; Bollimunta et al., 2012). It is difficult, however, to pinpoint
54 experimentally how much temporal integration is involved in the process (Ditterich, 2006), and the view
55 that single-trial decision-related neural activity is consistent with a diffusion-like process has been
56 challenged (Latimer et al., 2015).

57 More recently, confidence in a perceptual decision has become the focus of scientific investigation.
58 Some studies suggest that a common mechanism could explain both the outcome of the decision as well
59 as the reported confidence (Kiani and Shadlen, 2009; Kiani et al., 2014), while other reports have
60 focused on dissociations between subjective confidence and objective decision accuracy (see Rahnev
61 and Denison (2018) for a review). When making binary decisions, the choice and the associated
62 confidence fully describe the outcome of the decision process. When making decisions between more
63 than two alternatives, the decisionmaker could also have knowledge about how well the sensory
64 evidence supported the unchosen options.

65 Here we ask whether human subjects have access to information about the “relative desirability” of the
66 unchosen options when making perceptual decisions between more than two alternatives and, if so,
67 whether one can provide a quantitative explanation for the distribution of reported second guesses. We
68 used a modified version of the 3-alternative forced choice (3AFC) version of the multi-component
69 Random Dot Motion (RDM) direction discrimination task introduced in Niwa and Ditterich (2008).
70 Briefly, the subject watches an RDM stimulus that simultaneously contains coherent motion in three
71 different directions, all separated by 120 deg. The strength of each motion component is chosen
72 randomly. The observer has to determine the strongest motion component and indicate its direction
73 with an eye movement. The choice and the associated RT are recorded. For this study, subjects were
74 instructed to also report a second guess with a second eye movement. We asked the observers to
75 indicate which of the remaining two options they would rather bet on, assuming they got their primary
76 choice wrong. Once both the primary choice and the second guess had been registered, auditory
77 feedback about the accuracy of the primary choice was provided. Subjects did not receive feedback on
78 their second guess. The task is illustrated in Figure 1. Further details regarding the experimental design
79 can be found in Materials and Methods.

80 Here we demonstrate that the second guess is clearly informed by the sensory evidence and that a
81 single integration-to-threshold model can explain the distribution of primary choices, associated RTs,
82 and the distribution of second guesses. This suggests that the decisionmaker has access to how much
83 sensory evidence had been accumulated for options other than the chosen one at the time when the
84 decision was made. We also consider alternative models and show that the second-best explanation for
85 the data is provided by a model that starts a new decision process between the remaining alternatives
86 when the primary decision is made and reads out the decision variable after a fixed amount of time.

87

88

89 **MATERIALS AND METHODS**

90 Experimental Design and Statistical Analyses

91 *Human Subjects*

92 The study was approved by the UC Davis Institutional Review Board. After giving their informed consent,
93 seven UC Davis undergraduate students (4 females, 3 males) with normal or corrected-to-normal vision
94 participated in the experiment. Each of the subjects completed at least five experimental sessions with a
95 minimum of 300 valid decision trials each.

96

97 *Experimental Setup*

98 The subjects sat in front of a 22" flat-screen CRT video monitor (ViewSonic P225f; viewing distance:
99 60 cm) with their head on a chin and forehead rest. The visual stimuli were generated by a Macintosh
100 G4 computer running Mac OS 9, MATLAB (The Mathworks, Natick, MA), and the Psychophysics Toolbox
101 (Brainard, 1997; Pelli, 1997) at a frame rate of 75 Hz. The experiment was controlled and the data were
102 collected by an Intel Pentium IV computer running QNX (Ottawa, ON, Canada) and a modified version of
103 REX (Laboratory of Sensorimotor Research, National Eye Institute).

104 Eye movements were monitored using a monocular IR video eye tracker with chinrest-mounted optics
105 (Series 5000, Applied Science Laboratories, Bedford, MA) operating at 240 Hz. Prior to each
106 experimental session the eye tracker was calibrated using repeated fixation of nine calibration targets
107 with horizontal eccentricities of -10, 0, and +10 deg and vertical eccentricities of -7.5, 0, and +7.5 deg.

108

109

110 *Experimental Task and Visual Stimulus*

111 The experimental task is illustrated in Fig. 1. Each trial started with the presentation of a central fixation
112 mark (diameter: 0.3 deg). The measured fixation location had to remain within 2.5 deg of the center of
113 the screen throughout the trial (up to the saccadic response). After 250 to 500 ms of stable fixation,
114 three targets (diameter: 0.5 deg) appeared on the screen, all located on a virtual circle around the
115 fixation mark with a radius of 8.0 deg. The target locations were chosen randomly (with equal spacing)
116 at the beginning of an experimental sessions and did not change throughout the session. After another
117 random delay of 250 to 500 ms, a multi-component random-dot pattern was presented at the center of
118 the screen (diameter: 5.0 deg).

119 In the original version of the stimulus (as used, e.g., in Shadlen and Newsome, 2001; Roitman
120 and Shadlen, 2002; Palmer et al., 2005) a certain fraction of the dots (defined as the coherence of the
121 stimulus) was moving coherently in a particular direction, whereas the remaining dots were flickering
122 randomly. Our multi-component random-dot pattern had up to three coherent motion components
123 embedded. Thus, there were four subpopulations of dots: one was moving coherently in a particular
124 direction θ (aligned with one of the choice targets; fraction of dots defined by the coherence of the first
125 component), another one was moving coherently in the direction $\theta + 120^\circ$ (fraction defined by the
126 coherence of the second component), a third one was moving coherently in the direction $\theta + 240^\circ$
127 (fraction defined by the coherence of the third component), and the remaining dots were flickering
128 randomly. The stimulus is therefore described by a set of three coherences. Which of the four
129 subpopulations a particular dot belonged to, changed randomly over time. As a consequence, the
130 stimulus is not perceived as an overlay of several transparent layers of motion that could be easily
131 separated, but as a mixture of different motion components. See, e.g., Treue et al. (2000) for a
132 discussion of transparent random-dot motion stimuli. Corresponding pairs of dots, responsible for the

133 percept of apparent motion, were presented with a temporal separation of 40 ms (3 video frames). The
134 coherently moving dots had a speed of 6 deg/s, the dot density was $16.7 \frac{\text{dots}}{\text{deg}^2 \cdot \text{s}}$, and each dot was a
135 little filled square with an edge length of 0.1 deg. On each trial, the set of coherences was randomly
136 selected from a list of 51 possible coherence combinations ranging from 0 to 40% each. The full list can
137 be found in Table 1.

138
139 The subjects were instructed to identify the direction of the strongest motion component and to make a
140 saccadic eye movement to the associated choice target (aligned with the identified direction of motion).
141 They were allowed to watch the stimulus for as long as they wanted (up to 5 s) and to respond
142 whenever they were ready. The motion stimulus disappeared from the screen as soon as the eye left the
143 central fixation window. Subjects were further instructed to indicate with a second saccadic eye
144 movement to one of the two remaining choice targets, which of the remaining options they would
145 rather bet on as a second guess, assuming they got their first choice wrong. After each trial they
146 received auditory feedback as to whether they had picked the correct target in their primary choice. In
147 case the stimulus did not have one strongest motion component, the computer randomly identified one
148 of the targets as being the correct one. No feedback was given on the second guess.

149 In order to complete a trial successfully (“valid trial”), the subject had to maintain accurate fixation until
150 the random-dot pattern appeared. Once central fixation was broken, the eye position had to be within
151 3 deg of one of the three choice targets within 100 ms and had to stay on this target (primary choice) for
152 at least 200 ms. At this point, a neutral sound was played, indicating that the primary choice had been
153 registered, but not providing any information about its accuracy yet. At most 3 s later, the eye position
154 had to be within 3 deg of one of the remaining choice targets and had to stay on this target (second

155 guess) for at least 200 ms. At this point, auditory feedback was given about the accuracy of the primary
156 choice, which indicated to the subject that the trial had been registered as a valid trial.

157

158 *Data Analysis*

159 For analyzing the data, we collapsed across different target locations. Thus, we only worked with the 15
160 unique sets of coherences (eliminating the permutations) and whether the subject picked the target
161 associated with the strongest motion component, the one associated with the intermediate component,
162 or the one associated with the weakest component. We analyzed the pooled data across subjects to
163 have a robust number of trials for each experimental condition. Since we only work with mean RTs in
164 this study, we were not concerned about variability in RT across subjects potentially affecting the shape
165 of RT distributions.

166 RT was defined as the time between the appearance of the random-dot stimulus and the breaking of
167 central fixation. We did not analyze the timing of the second guess as subjects had to wait for their
168 primary choice to be registered by the computer before they could report their second guess. Thus, the
169 timing of the second guess was largely externally imposed.

170

171 Computational Models

172 *Model of the neural representation of the sensory stimulus*

173 The mean response of a population of motion-sensitive neurons to a 3-component random-dot stimulus
174 with coherences c_1 (in the preferred direction of the pool), c_2 , and c_3 was modeled to be of the form

175
$$\bar{s}_1 = \frac{g \cdot \left[c_1 + k_n \cdot \left(1 - \sum_{i=1}^3 c_i \right) \right]}{1 + k_s \cdot (c_2 + c_3)}$$

176 where g is the overall gain of the sensory response (relationship between neural activity and motion
 177 strength). The two additive terms in the brackets reflect the two linear response components: the first
 178 describes the response to the coherent motion in the preferred direction, the second describes the
 179 response to the noise dots. The term in parenthesis reflects the proportion of noise dots in the stimulus.
 180 k_n is the relative gain of the response to the noise dots compared to the response to an identical
 181 fraction of dots moving coherently in the preferred direction. The term in the denominator reflects the
 182 divisive normalization. Since the term in the numerator accurately describes the response to a single-
 183 component stimulus, only the coherences of motion components with directions other than the
 184 preferred one are present in the denominator. For simplicity, we have chosen a linear term, with k_s
 185 describing the gain/strength of the divisive normalization (Niwa and Ditterich, 2008).

186 In general, the mean responses of each of the three task-relevant sensory pools can be written as

187
$$\bar{s}_j = \frac{g \cdot \left[c_j + k_n \cdot \left(1 - \sum_{i=1}^3 c_i \right) \right]}{1 + k_s \cdot \sum_{i \neq j} c_i}$$

188 The variances of the three sensory responses were modeled as

189
$$\sigma_{s_j}^2 = k_v \cdot \bar{s}_j$$

190 We described the outputs of the sensory pools as normal random processes to be able to treat the
 191 decision process as a standard diffusion process (based on Brownian motion), which is reasonable if the
 192 pools are not too small.

193

194 *Model of the decision process*

195 In principle, we would have to treat the race between the three integrators mathematically as a
196 3-dimensional diffusion process. However, for the 2AFC case, the decision process has often been
197 described as a 1-dimensional diffusion process with two boundaries instead of a 2-dimensional diffusion
198 process. This simplification can be done when one assumes that the two signals that are accumulated by
199 the two integrators are only different in sign, but identical in absolute value. Such a situation would
200 result from all of the contributions that a particular pool of sensory neurons makes to the net evidence
201 signals having the same origin. If we make the same assumption in our model, we can also reduce the
202 dimensionality of the problem. We can write the three evidence signals as

$$\begin{aligned} e_1 &= s_1 - \frac{1}{2}s_2 - \frac{1}{2}s_3 \\ e_2 &= s_2 - \frac{1}{2}s_1 - \frac{1}{2}s_3 \\ e_3 &= s_3 - \frac{1}{2}s_1 - \frac{1}{2}s_2 \end{aligned}$$

204 e_3 can be rewritten as

$$e_3 = -\left(s_1 - \frac{1}{2}s_2 - \frac{1}{2}s_3\right) - \left(s_2 - \frac{1}{2}s_1 - \frac{1}{2}s_3\right) = -e_1 - e_2$$

206 Thus, if e_1 and e_2 are known, e_3 is known. In our model, each of the three evidence signals is integrated
207 over time (see Fig. 2):

$$i_j(t) = \int_0^t e_j(\tau) d\tau$$

209 Since integration is a linear operation, if i_1 and i_2 are known, i_3 is also known. We can therefore rewrite
210 the decision criterion for choosing the 3rd alternative:

$$\begin{aligned}
& i_3 > 1 \\
211 \quad & -i_1 - i_2 > 1 \\
& i_2 < -i_1 - 1
\end{aligned}$$

212 Thus, the third integrator exceeding a value of 1 is equivalent to crossing another linear boundary in the
213 $i_1 - i_2$ plane (for an illustration see Niwa and Ditterich (2008), Fig. 3C). The diffusion process always starts
214 at (0;0) and stops when one of the three boundaries is crossed: $i_1 = 1$ is the decision boundary for the
215 1st alternative, $i_2 = 1$ is the boundary for the 2nd alternative, and $i_2 = -i_1 - 1$ is the boundary for the 3rd
216 alternative.

217 The 2-dimensional diffusion process is described by a drift vector and a covariance matrix. The drift
218 vector is given by $\begin{bmatrix} \bar{e}_1 \\ \bar{e}_2 \end{bmatrix}$, the means of the first two evidence signals. Since $\begin{bmatrix} e_1 \\ e_2 \end{bmatrix}$ can be calculated as

$$219 \quad \begin{bmatrix} e_1 \\ e_2 \end{bmatrix} = \begin{bmatrix} 1 & -\frac{1}{2} & -\frac{1}{2} \\ -\frac{1}{2} & 1 & -\frac{1}{2} \end{bmatrix} \cdot \begin{bmatrix} s_1 \\ s_2 \\ s_3 \end{bmatrix}$$

220 $\begin{bmatrix} \bar{e}_1 \\ \bar{e}_2 \end{bmatrix}$ is given by

$$221 \quad \begin{bmatrix} \bar{e}_1 \\ \bar{e}_2 \end{bmatrix} = \begin{bmatrix} 1 & -\frac{1}{2} & -\frac{1}{2} \\ -\frac{1}{2} & 1 & -\frac{1}{2} \end{bmatrix} \cdot \begin{bmatrix} \bar{s}_1 \\ \bar{s}_2 \\ \bar{s}_3 \end{bmatrix}$$

222 The covariance matrix Σ can be calculated as

$$\begin{aligned}
\Sigma &= \begin{bmatrix} 1 & -\frac{1}{2} & -\frac{1}{2} \\ -\frac{1}{2} & 1 & -\frac{1}{2} \end{bmatrix} \cdot \begin{bmatrix} \sigma_{s_1}^2 & 0 & 0 \\ 0 & \sigma_{s_2}^2 & 0 \\ 0 & 0 & \sigma_{s_3}^2 \end{bmatrix} \cdot \begin{bmatrix} 1 & -\frac{1}{2} \\ -\frac{1}{2} & 1 \\ -\frac{1}{2} & -\frac{1}{2} \end{bmatrix} = \\
&= \begin{bmatrix} \sigma_{s_1}^2 + \frac{1}{4}\sigma_{s_2}^2 + \frac{1}{4}\sigma_{s_3}^2 & -\frac{1}{2}\sigma_{s_1}^2 - \frac{1}{2}\sigma_{s_2}^2 + \frac{1}{4}\sigma_{s_3}^2 \\ -\frac{1}{2}\sigma_{s_1}^2 - \frac{1}{2}\sigma_{s_2}^2 + \frac{1}{4}\sigma_{s_3}^2 & \frac{1}{4}\sigma_{s_1}^2 + \sigma_{s_2}^2 + \frac{1}{4}\sigma_{s_3}^2 \end{bmatrix} = \\
&= k_v \cdot \begin{bmatrix} \bar{s}_1 + \frac{1}{4}\bar{s}_2 + \frac{1}{4}\bar{s}_3 & -\frac{1}{2}\bar{s}_1 - \frac{1}{2}\bar{s}_2 + \frac{1}{4}\bar{s}_3 \\ -\frac{1}{2}\bar{s}_1 - \frac{1}{2}\bar{s}_2 + \frac{1}{4}\bar{s}_3 & \frac{1}{4}\bar{s}_1 + \bar{s}_2 + \frac{1}{4}\bar{s}_3 \end{bmatrix}
\end{aligned}$$

224

225 *Model of the second choice based on accumulated evidence at or shortly after the time of the first*
226 *threshold crossing*

227 The integrator crossing the decision threshold first determines the primary choice and the decision time.
228 We propose that the state of the remaining integrators at the time when the winning integrator crosses
229 threshold can be used to determine the second guess. The higher value of the two remaining integrators
230 determines the second choice. For example, if the second integrator crossed the threshold first, the
231 states of the first and the third integrator at this particular time would be compared, and the larger
232 value would determine the second guess. As pointed out above, when working with a 2-dimensional
233 stochastic process, the two dimensions correspond to the states of the first two integrators. The state of
234 the third integrator can be calculated as $i_3 = -i_1 - i_2$.

235 While the first passage time problem could be solved numerically (see Ditterich, 2006, section B.5 and
236 Niwa and Ditterich, 2008), we also needed the predictions for the distribution of second choices.
237 Therefore, we discretized the 2-dimensional diffusion process (time step: 5 ms) and simulated 50,000
238 trials per experimental condition. The MATLAB function `OU_2D_3B_SIM_SC.M`, which has been used for
239 performing the model calculations, is part of the Stochastic Integration Modeling Toolbox (SIMT; written
240 by JD), which can be downloaded from <https://www.github.com/peractionlab/StochInt>.

241 To determine whether the second guess might have been informed by sensory evidence that arrived at
242 the decision process after the decision threshold had been crossed, we allowed the integration process
243 to continue for a fixed amount of time after the threshold crossing and then read out and compared the
244 states of the integrators that had not won the race to threshold. The MATLAB function used for this
245 purpose, OU_2D_3B_SIM_SC_ADD_TIME.M, is also part of SIMT. To quantify the deviation between
246 predicted and observed second guesses, we calculated the sum of the squared differences between
247 predicted and observed relative frequencies.

248

249 *Model of the second choice based on two successive threshold crossings*

250 We also considered a model where the integration process continues after the first threshold crossing,
251 until a second (different) bound is crossed. The first threshold crossing determines the first choice, the
252 second threshold crossing the second choice and the decision time. In contrast to our original model, to
253 give this model more flexibility, the integration of sensory evidence was allowed to be leaky (the time
254 constant of integration was an additional free model parameter), and the bounds were allowed to
255 collapse over time. We used the same logistic function as in Ditterich (2006):

$$256 \quad A(t) = \frac{1}{1 + \exp(s \cdot (t - d))} + \frac{\exp(-s \cdot d)}{1 + \exp(-s \cdot d)}$$

257 t is the time into the decision process, and s and d are two additional free model parameters that
258 define the shape (slope) and the position (delay) of the collapsing bound. The MATLAB function
259 OU_2D_3B_TWO_CROSS_SIM.M, which was used for evaluating this model, is also part of SIMT.

260

261

262 *Models of the second choice based on two successive decision processes*

263 Another class of models involved starting a new decision process when the first threshold crossing
264 occurred, but only between the two alternatives that did not win the original race to threshold. For
265 example, assuming that i_2 crossed the threshold first, the second process would be set up as

$$e'_1 = s_1 - s_3$$
$$e'_2 = s_3 - s_1$$

267 If the integral of the first evidence signal crossed the threshold first, Direction 1 would be reported as
268 the second choice. If the integral of the second evidence signal crossed the threshold first, Direction 3
269 would be reported as the second choice. Since $e'_2 = -e'_1$, this second decision process can be treated as
270 a 1-dimensional drift-diffusion process with two boundaries. The decision time would be the total
271 duration of both decision processes. To give this model more flexibility, we allowed the decision
272 threshold of the second decision process to be lower than the decision threshold of the first decision
273 process. The second decision threshold was an additional free model parameter. The MATLAB function
274 `OU_2D_3B_1D_2B_SIM_SC.M`, which has been used for evaluating this model, is also part of SIMT.

275 Finally, we considered a model that also starts a second decision process when the first threshold
276 crossing occurs, but it does not wait for a second threshold crossing. The second decision process
277 unfolds for a fixed amount of time and is then read out. The sign of the current state of the integrated
278 evidence (of the 1D process) determines the second choice. The MATLAB function
279 `OU_2D_3B_1D_FIXED_TIME_SIM_SC.M`, which was used for evaluating this model, is also part of SIMT.

280

281

282 *Model Fit*

283 The model parameters were identified by an optimization procedure based on the mean RTs. A
284 combination of a global pattern search (provided by MATLAB's Global Optimization Toolbox) and a
285 multi-dimensional simplex algorithm (provided by MATLAB's Optimization Toolbox) was used to
286 minimize the sum of the squared differences between the mean RTs in the data and the mean RTs
287 predicted by the model, taking the standard errors of the estimated means into account. We used the
288 mean RTs for each combination of coherences, regardless of choice (15 data points). For the model
289 these were obtained by calculating a weighted sum of the predicted mean RTs for the different choices
290 based on the predicted probabilities of these choices.

291

292 **RESULTS**

293 We used 11,060 valid decision trials from seven subjects for analysis and modeling. The overall accuracy
294 of the primary choice was 72% (chance level would be 33% for a 3AFC task), which provided us with
295 7,951 correct trials and 3,109 error trials for further analysis. How the primary choice and the associated
296 RT depended on the presented stimulus was similar to what we had reported in Niwa and
297 Ditterich (2008) and will be presented in the context of a computational model below.

298

299 *Second guesses in perceptual decision-making are informed by sensory evidence*

300 To test whether subjects are able to make an informed second guess, we analyzed the error trials and
301 quantified how often subjects reported what would have been the correct choice as their second guess.
302 If subjects just guessed randomly, this should not deviate significantly from chance (50%). The correct
303 option, however, was reported as the second guess in 63% of the error trials, which is highly significantly

304 above chance ($p < 10^{-6}$; binomial test). This indicates that the second guess was clearly informed by the
305 sensory evidence provided by the motion stimulus.

306

307 *A computational model that can explain primary choices and associated RTs*

308 To gain more insight into what information the second guesses were based on, we resorted to
309 computational modeling. In Niwa and Ditterich (2008) we presented an integration-to-threshold model
310 that was able to explain the distribution of choices in the 3-choice multi-component RDM direction
311 discrimination task as well as the associated RTs. Briefly, in a stochastic process, we modeled three pools
312 of motion-sensitive neurons (for each of the possible directions). Each of these pools had a strong linear
313 response to coherent motion in its preferred direction, a weak linear response to the randomly moving
314 dots in the stimulus, and divisive normalization based on how much coherent motion the stimulus
315 contained driving the other pools. The variance of each pool's output scaled linearly with its mean. The
316 net sensory evidence for each direction, calculated as the difference between one pool's activity and the
317 average activity of the other two, was then fed into an integrator, one for each possible choice.
318 Whichever integrator reached a constant decision threshold first determined the choice, and the time of
319 crossing the decision threshold the decision time. RT was modeled as the sum of the decision time and a
320 fixed residual time, capturing the time needed for aspects of the task other than the decision itself, e.g.,
321 initiating an eye movement for reporting the choice. The structure of the model is shown in Figure 2.
322 Further details can be found in Materials and Methods.

323 If adding the secondary task of reporting a second guess did not alter the way subjects made their
324 primary choice, the same model should still be able to capture the primary choice data and associated
325 RTs from this experiment. To test this, we fitted the model (5 free parameters) to the mean RT data. The
326 result of this fit is shown in Figure 3. Filled circles represent the data (with 95% confidence intervals,

327 calculated according to the method proposed by Goodman, 1965), lines the model. The motion strength
328 of the strongest motion component in the stimulus is plotted on the horizontal axis, the color of
329 symbols/lines reflects the strength of the other two motion components. The model clearly captures the
330 structure of the mean RT data. If the model were perfect, at least 95% of the evaluated model mean RTs
331 would be expected to be within the 95% confidence intervals associated with the data. Our model is
332 close to that: 13 of the 15 mean RTs (87%) are inside, the two that are outside are still close to the
333 confidence intervals. The estimated model parameters are summarized in Table 2.

334 To further test whether the model can explain the primary choice data, we compared the model's
335 prediction for the distribution of primary choices with the actual distribution from the experiment
336 (Figure 4). These data have not been used yet, because the model had only been fitted to mean RT data.
337 The plotting conventions are similar to Figure 3. Circles indicate correct choices, squares choices of the
338 direction that had intermediate support, and diamonds choices of the direction that had the weakest
339 support. A perfect model would predict probabilities, at least 95% of which would be expected to be
340 within the 95% confidence intervals associated with the data. While our model is not perfect, 18 of the
341 23 probabilities (78%) are inside, the five that are outside are still close to the confidence intervals. The
342 good agreement between data and model predictions indicates that the model introduced in Niwa and
343 Ditterich (2008) is still able to explain the primary choice data and associated RTs from the current
344 experiment. Thus, asking subjects to report a second guess apparently did not alter the structure of the
345 decision process.

346

347 *The same computational model can also explain second guesses*

348 We have demonstrated earlier that subjects can produce informed second guesses when making
349 perceptual decisions between multiple alternatives, but can we gain insight into what governs these

350 second guesses? The idea behind the highly successful integration-to-threshold models in perceptual
351 decision-making is that decisionmakers accumulate sensory evidence for each of the possible choices
352 until the accumulated evidence for one of them exceeds a decision threshold. How could a subject make
353 an informed second guess in this framework? Assume the decisionmaker had access to the states of the
354 integrators that did not win the race at the time of the threshold-crossing. What should the distribution
355 of second guesses look like if subjects reported the integrator with the overall second-highest
356 accumulated evidence as their second guess, or, equivalently, the option with the larger accumulated
357 evidence out of the two remaining ones? We took the model, which had been fitted to the mean RTs
358 associated with the primary choice and was able to explain the distribution of primary choices, and
359 obtained the expected distributions of second guesses based on the overall second-highest accumulated
360 evidence.

361 A comparison between the predicted distributions of second guesses and the actual data on correct
362 trials is shown in Figure 5. Symbols again represent the data (and 95% confidence intervals), lines reflect
363 the model predictions. On correct trials, by definition, subjects have already reported the correct option
364 as their primary choice. The correct option is therefore no longer available as a second guess. The
365 relative frequency of reporting the correct option as the second guess (filled circles) has to be zero. The
366 only interesting cases are those where the two weaker motion components had different motion
367 strengths (purple and cyan). Squares indicate how often subjects reported the direction with the
368 intermediate motion strength as their second guess, diamonds how often the weakest motion
369 component was reported.

370 The same comparison, but now for error trials, is shown in Figure 6. In this case, the correct option can
371 be reported as the second guess, and we had already seen earlier that, across experimental conditions,
372 it was chosen more frequently than chance. The figure shows this relative frequency broken down by
373 experimental condition (circles), adds the relative frequencies of reporting each incorrect option as the

374 second guess (squares and diamonds), and provides the model predictions for comparison. Why, in
375 contrast to the plots we had seen so far, are the squares below the diamonds in this figure? When
376 reporting their primary choice, subjects were more likely to make an error in favor of the motion
377 component with intermediate support rather than picking the weakest component (see squares and
378 diamonds in Figure 4). The weakest component (diamonds) was therefore available as an option for the
379 second guess in substantially more error trials than the component with the intermediate support
380 (squares), which explains why it was overall chosen more frequently. And why does the probability of
381 reporting the direction of the strongest motion component (blue circles/line) not keep increasing
382 monotonically as a function of motion strength? To make an error in a trial with only a single motion
383 component with 40% coherence in the first place, the accumulated evidence for this direction has to be
384 unusually low. As a consequence, since the second guess is based on the same accumulated evidence,
385 there is also not a sufficient amount of evidence to support choosing this direction as the second guess.
386 A perfect model would again predict probabilities, at least 95% of which would be expected to be within
387 the 95% confidence intervals associated with the data. Across both correct and error trials and not
388 counting the zero-probability events, 26 of the 31 predicted probabilities (84%) are inside, the five that
389 are outside are still pretty close to the confidence intervals. Thus, there is good agreement between the
390 data and model predictions, indicating that the reported second guesses are consistent with the idea
391 that the decisionmaker has access to information about how much sensory evidence had been
392 accumulated for competing unchosen options at the time when sufficient evidence had been collected
393 to commit to a primary choice.

394 In summary, a computational model with only five free parameters can account for 15 mean RTs, 16
395 relative frequencies for the primary choice (not counting the 7 trivial cases of uniform choice
396 distributions when all motion components are equally strong and the relative frequency of choosing the
397 third option having to be one minus the sum of the relative frequencies of choosing the first or the

398 second option), and 18 relative frequencies for the second guess, again excluding the trivial cases. This
399 strongly suggests that the primary choice and the second guess are produced by a common integration-
400 to-threshold decision process.

401

402 *Second guesses are best explained by the states of the integrators shortly after threshold crossing*

403 While the motion stimulus disappeared from the screen when the saccade for reporting the primary
404 choice was detected, there is a delay between the decision threshold crossing and the saccade onset,
405 and some stimulus information is also still in the visual cortical processing pipeline. In the decision
406 confidence literature, it has been proposed that the decision confidence, which is usually reported after
407 the choice, could be informed by sensory evidence that is processed after the choice has been made
408 (Pleskac and Busemeyer, 2010; Moran et al., 2015). To determine whether additional sensory evidence
409 might have contributed to the reported second guesses in our experiment, we created a variant of the
410 model, where the evidence accumulation was allowed to continue for a fixed period of time after the
411 decision threshold had been crossed, before the non-winning integrators were read out to determine
412 the second choice. Figure 7A shows the deviation between predicted and observed second guesses as a
413 function of the additional integration time. Since the calculated points (blue circles) are simulation-
414 based and therefore slightly noisy, we added a robust polynomial interpolation (solid black line). The
415 best match between predicted and observed second guesses (discrepancy of 0.027) is obtained for an
416 additional integration time of 40 ms (dashed vertical line), i.e., when the integrators are read out shortly
417 after the threshold crossing. The discrepancy clearly increases for longer additional integration times.
418 Thus, the second guesses seem to be affected by a small amount of sensory evidence that is processed
419 after the primary choice has been determined, but still largely rely on the same information, as typical
420 decision times in our experiment are an order of magnitude larger. The predicted relative frequencies of

421 second guesses for a model with 40 ms of additional integration time are shown in Figures 7B and C.
422 There is no major qualitative difference between these plots and Figures 5 and 6, the match between
423 model predictions (lines) and data (symbols) is just slightly better.

424

425 *A model waiting for the same decision process to cross a second threshold can be ruled out*

426 To determine whether the second guesses could also be explained by alternative mechanisms that do
427 not require reading out and comparing the accumulated evidence for the options that did not win the
428 race to threshold, we considered several alternative models. First, we evaluated the possibility that the
429 decision process could continue after the first threshold crossing until a second (different) threshold is
430 crossed. The first threshold crossing would determine the primary choice, the second threshold crossing
431 the second choice and the decision time. One can imagine that in situations where there is much
432 stronger evidence for one particular choice compared to the other alternatives, such a second threshold
433 crossing is unlikely to occur within a reasonable amount of time, in particular when the integration is
434 perfect, and the decision bounds are fixed. We therefore also considered mechanisms with leaky
435 integration and collapsing decision bounds (Ditterich, 2006). It turns out, however, that this class of
436 models, even in the presence of leaky integration and collapsing bounds, makes one key qualitative
437 prediction: decision times should increase, rather than decrease, when the evidence gets stronger. As a
438 consequence, the best mean RT fit that can be obtained is largely flat as a function of motion strength,
439 and the remaining error is about 6 times as large as the one for the fit shown in Fig. 3. Figure 8A shows
440 this fitting attempt. This class of models can therefore be ruled out as an alternative explanation.

441

442

443 *A model based on a second integration-to-threshold process for determining the second choice makes*
444 *less accurate predictions for the distribution of second guesses*

445 We also considered the possibility that, as soon as the first threshold crossing occurs, a new decision
446 process, only as a 2AFC between the two remaining options, is started. A threshold crossing of the
447 second decision process would then determine the second choice and the decision time. When
448 enforcing the same decision threshold as in the primary decision process, the remaining error after the
449 mean RT fit is more than an order of magnitude larger than the one for the fit shown in Fig. 3. We
450 therefore considered the possibility that the decision threshold for the second decision process could be
451 lower. The mean RT fit reveals that the threshold would have to be very close to zero to be able to
452 account for the pattern of RTs. A fit with a decision threshold of 0.052 (compared to 1 in the case of the
453 first decision process) resulted in a remaining error that was only slightly larger than the one for the fit
454 shown in Fig. 3. We therefore determined the predicted second guesses for this model (shown in
455 Figure 8B and C). The discrepancy between predicted and observed second guesses, following the same
456 convention as the one used in Fig. 7A, was 0.129 (red dashed line in Fig. 8D), about five times as big as
457 the one for the model shown in Fig. 7B and C. Thus, this model also cannot capture the data pattern as
458 well as our original model.

459

460 *A model based on a second, fixed-duration decision process for determining the second choice provides*
461 *the second-best explanation for the distribution of second guesses*

462 As a final possibility, we considered that the second decision process might not be terminated by a
463 threshold crossing, but rather end after a fixed amount of time. The process would be read out at that
464 point, and the sign of the accumulated evidence would determine the second choice. The discrepancy
465 between predicted and observed second guesses for this model, as a function of the duration of the

466 second decision process, is shown in Figure 8D. Since the calculated points (blue circles) are simulation-
467 based and therefore slightly noisy, we again added a robust polynomial interpolation (solid blue line).
468 The best match is observed for an integration time of 70 ms, but the discrepancy is still 0.081, about
469 three times as big as the one for the model shown in Fig. 7B and C (solid black in Fig. 8D). This model's
470 predictions for the second guesses are shown in Figures 8E and F. In contrast to our original model,
471 which predicted the nonmonotonic relationship between motion strength and the probability of
472 choosing the strongest motion component as the second guess on error trials (blue circles in Fig. 8F),
473 this model predicts a monotonic relationship (blue line). This difference results from the fresh start of
474 evidence accumulation in the second decision process, rather than the second guess being substantially
475 affected by the accumulated evidence that led to the primary choice. Since 70 ms are needed for the
476 second integration process, the residual time would be reduced to 593 ms in this case. While this model
477 provides the second-best explanation, our original model still provides the better explanation for the
478 observed pattern of second guesses.

479

480 **DISCUSSION**

481 We asked human subjects to make a perceptual decision among three alternatives and to report not
482 only their primary choice, but also a second guess. Our data indicate that this second guess is not
483 random, but clearly informed by the sensory evidence. A single integration-to-threshold model can not
484 only explain the distribution of primary choices and the associated RTs, but also the distribution of
485 second guesses. This suggests that the second guess is generated based on largely the same
486 accumulated evidence that is also used to produce the primary choice. The second guess appears to be
487 governed by the ranking of the amounts of evidence that have been accumulated by the integrators that
488 did not win the race to threshold, which are apparently accessible.

489 We also considered alternative models. The only other model that was able to largely capture the data
490 pattern, although not as well as the model based on reading out the states of the integrators that had
491 not crossed the decision threshold yet shortly after the winning integrator crossing its threshold, was a
492 model based on starting a new decision process when the threshold crossing determining the primary
493 choice occurred. The process had to be set up as a decision between the remaining alternatives and
494 read out after a fixed amount of time (about 70 ms).

495

496 *Relationship with decision confidence*

497 Human subjects can not only report their choice when making a perceptual decision, but also express a
498 level of confidence in their decision. A substantial body of literature has been devoted to how well
499 calibrated this decision confidence is and how it might be computed. Ideally, the level of confidence
500 should match the accuracy of the decision. However, this is typically not the case, and human subjects
501 have been reported to be either under- or overconfident, depending on the difficulty of the decision
502 (see Rahnev and Denison, 2018 for a review). Confidence clearly is informed by the available sensory
503 evidence, but how? Vickers (1979) suggested that it depends on the balance of evidence. The more
504 dissimilar the amounts of evidence in favor of the available options are at the time of making a decision,
505 the more confident the observer can be about the choice. This information can be extracted from the
506 decision process itself. While the idea is incompatible with the popular 1-dimensional drift-diffusion
507 model for 2-alternative forced choices, which is equivalent to a race between two accumulators that
508 receive perfectly anti-correlated instantaneous net evidence and, as a consequence, always has the
509 losing integrator in an identical state when the winning integrator exceeds the decision threshold, it can
510 be applied to alternative models. For example, Ditterich (2006) demonstrated that a model based on
511 partially anti-correlated accumulators provides a better account of decision-related activity in the

512 parietal association cortex of monkeys performing a perceptual decision task. Neurons coding for the
513 losing alternative do not show a stereotyped activity level when the neurons coding for the winning
514 alternative reach threshold. This information could be used to inform confidence. Moreno-Bote (2010)
515 formalized how confidence can be extracted from diffusion models with partially correlated integrators.
516 An alternative mechanism was proposed by Smith and Vickers (1988). According to their model, only
517 one of the integrators is updated at a particular time, the one receiving positive instantaneous net
518 sensory evidence, which also results in the losing accumulator being in different states when the
519 winning accumulator reaches threshold.

520 Gaining neurophysiological insights into the neural mechanism underlying decision confidence from
521 animal experiments is challenging, as animals cannot be asked directly to provide an explicit confidence
522 rating. However, animal tasks have been developed, which require the animal to produce a behavior
523 that should be informed by decision confidence (see Hanks and Summerfield, 2017 for a review). For
524 example, Kiani and Shadlen (2009) trained monkeys to make a perceptual decision between two
525 alternatives. In a random subset of trials, the researchers offered a third option, a sure bet resulting in a
526 smaller, but certain reward, whereas the animals could gain a larger reward if they engaged in a choice
527 and reported the correct option. The animals were more likely to choose the sure bet the weaker the
528 sensory evidence (motion coherence) was and the shorter they were allowed to watch the motion
529 stimulus. Importantly, decision-related neurons in parietal association cortex that have the signature of
530 carrying accumulated evidence showed either strong or weak activation when the animal engaged in a
531 choice, but intermediate activation when opting for the sure bet, suggesting that the information
532 encoded in these neurons does not only govern choice, but also inform confidence. The study further
533 suggested that decision confidence does not only depend on accumulated evidence, but also on elapsed
534 time, which was confirmed explicitly in a later human psychophysics experiment (Kiani et al., 2014) and
535 is also formalized in Moreno-Bote's (2010) model. Animal experiments on decision confidence have

536 received some criticism, primarily claiming that the tasks could potentially be solved without requiring
537 any meta-cognition, for example, by treating tasks with a sure bet as a multi-alternative decision task
538 (Insabato et al., 2016, 2017). However, Kepecs and Mainen (2012) pointed out that the same scrutiny
539 should then also be applied to human tasks.

540 The view that confidence is governed by the same information that determines the choice and, in
541 particular, by the balance of evidence has been challenged by experiments that found that confidence
542 primarily relies on response-congruent evidence (Zylberberg et al., 2012; Maniscalco et al., 2016). The
543 authors reported that, while choices in their experiments were governed by the balance of evidence,
544 confidence was primarily determined by the amount of evidence for the chosen option and largely
545 insensitive to the amount of evidence for the non-chosen alternative. Dual stage or second-order
546 models are also at odds with the idea that choice and confidence rely on the same information (Pleskac
547 and Busemeyer, 2010; Moran et al., 2015; Fleming and Daw, 2017). These models posit that confidence
548 ratings rely on a post-decision process that is informed by the outcome of the decision process, but not
549 exclusively.

550 Different studies have therefore found the information upon which choice and decision confidence are
551 based to overlap to varying degrees. We have addressed a similar question for the mechanism
552 underlying second guesses. Our results indicate that the distribution of second guesses is most
553 compatible with a decision mechanism that largely uses the same accumulated evidence for
554 determining both the primary and the second choice. We found the best match between model
555 predictions and data, when the decision process was allowed to continue for a very short period of time
556 (compared to typical decision times in our experiment), about 40 ms, after the threshold crossing
557 determining the primary choice, before the states of the remaining integrators are read out to
558 determine the second choice.

559

560 *Second guessing in other cognitive functions*

561 In 1961, Signal Detection Theory (SDT) was still in its infancy and competing with the prevailing “high
562 threshold” model of sensory perception, Swets and colleagues published a paper proposing that a
563 second-choice paradigm in multi-interval signal detection could help distinguishing between the
564 competing ideas (Swets et al., 1961). However, second-choice paradigms have not been pursued further
565 in the area of perceptual decision-making, in particular not since the field has turned to sequential
566 sampling models to explain not only choices, but also decision times. Instead, Swets et al.’s proposal got
567 picked up in the memory literature, there typically referred to as a 4AFC-2R (four-alternative forced
568 choice with two responses) paradigm, as the field was also debating whether recognition memory was
569 best described by a threshold process or by a continuous memory strength process. Parks and
570 Yonelinas (2009) used a second-choice paradigm to gather experimental evidence beyond the Receiver
571 Operating Characteristic analysis that the field had relied on previously. Kellen and Klauer (2011)
572 followed up with a more detailed model-based analysis. Earlier, second guesses had already been used
573 to study mechanisms underlying the effect of misinformation on memory recall (Wright et al., 1996).
574 More recently, second guesses have also been used to study conflict detection mechanisms in reasoning
575 (Bago et al., 2019).

576

577 *Second guesses as a tool for studying knowledge about the decision process*

578 We have shown that human subjects can produce informed second guesses when making perceptual
579 decisions between multiple alternatives and that these second choices follow a distribution that would
580 be expected if they were governed by the relative amounts of accumulated net sensory evidence for
581 each option at the time of the largest accumulated evidence reaching a bound. Second-choice

582 paradigms therefore cannot only be used in the context of SDT, as they have in the past, but also with
583 accumulation-of-evidence frameworks. In addition to decision confidence, the study of second guesses
584 provides another useful tool for gaining insight into the decision process and what information a
585 decisionmaker has access to about the outcome of a decision, beyond the discrete choice. Similar to the
586 neurophysiological work on decision confidence, we expect future studies to be able to establish a link
587 between second guesses and underlying neural activity.

588

589 REFERENCES

- 590 Bago B, Raelison M, De Neys W (2019) Second-guess: Testing the specificity of error detection in the
591 bat-and-ball problem. *Acta Psychol (Amst)* 193:214-228.
- 592 Bollimunta A, Totten D, Ditterich J (2012) Neural dynamics of choice: single-trial analysis of decision-
593 related activity in parietal cortex. *J Neurosci* 32:12684-12701.
- 594 Brainard DH (1997) The Psychophysics Toolbox. *Spat Vis* 10:433-436.
- 595 Ditterich J (2006) Stochastic models of decisions about motion direction: behavior and physiology.
596 *Neural Netw* 19:981-1012.
- 597 Ditterich J (2010) A Comparison between Mechanisms of Multi-Alternative Perceptual Decision Making:
598 Ability to Explain Human Behavior, Predictions for Neurophysiology, and Relationship with
599 Decision Theory. *Front Neurosci* 4:184.
- 600 Fleming SM, Daw ND (2017) Self-evaluation of decision-making: A general Bayesian framework for
601 metacognitive computation. *Psychol Rev* 124:91-114.
- 602 Forstmann BU, Ratcliff R, Wagenmakers EJ (2016) Sequential Sampling Models in Cognitive
603 Neuroscience: Advantages, Applications, and Extensions. *Annu Rev Psychol* 67:641-666.

604 Goodman LA (1965) On Simultaneous Confidence Intervals for Multinomial Proportions. *Technometrics*
605 7:247-254.

606 Hanks TD, Summerfield C (2017) Perceptual Decision Making in Rodents, Monkeys, and Humans. *Neuron*
607 93:15-31.

608 Insabato A, Pannunzi M, Deco G (2016) Neural correlates of metacognition: A critical perspective on
609 current tasks. *Neurosci Biobehav Rev* 71:167-175.

610 Insabato A, Pannunzi M, Deco G (2017) Multiple Choice Neurodynamical Model of the Uncertain Option
611 Task. *PLoS Comput Biol* 13:e1005250.

612 Kellen D, Klauer KC (2011) Evaluating models of recognition memory using first- and second-choice
613 responses. *J Math Psychol* 55:251-266.

614 Kepecs A, Mainen ZF (2012) A computational framework for the study of confidence in humans and
615 animals. *Philos Trans R Soc Lond B Biol Sci* 367:1322-1337.

616 Kiani R, Shadlen MN (2009) Representation of confidence associated with a decision by neurons in the
617 parietal cortex. *Science* 324:759-764.

618 Kiani R, Corthell L, Shadlen MN (2014) Choice certainty is informed by both evidence and decision time.
619 *Neuron* 84:1329-1342.

620 Latimer KW, Yates JL, Meister ML, Huk AC, Pillow JW (2015) Single-trial spike trains in parietal cortex
621 reveal discrete steps during decision-making. *Science* 349:184-187.

622 Luce RD (1986) *Response Times: Their Role in Inferring Elementary Mental Organization*: Oxford
623 University Press.

624 Maniscalco B, Peters MA, Lau H (2016) Heuristic use of perceptual evidence leads to dissociation
625 between performance and metacognitive sensitivity. *Atten Percept Psychophys* 78:923-937.

626 Moran R, Teodorescu AR, Usher M (2015) Post choice information integration as a causal determinant of
627 confidence: Novel data and a computational account. *Cogn Psychol* 78:99-147.

628 Moreno-Bote R (2010) Decision confidence and uncertainty in diffusion models with partially correlated
629 neuronal integrators. *Neural Comput* 22:1786-1811.

630 Niwa M, Ditterich J (2008) Perceptual decisions between multiple directions of visual motion. *J Neurosci*
631 28:4435-4445.

632 Palmer J, Huk AC, Shadlen MN (2005) The effect of stimulus strength on the speed and accuracy of a
633 perceptual decision. *J Vis* 5:376-404.

634 Parks CM, Yonelinas AP (2009) Evidence for a memory threshold in second-choice recognition memory
635 responses. *Proc Natl Acad Sci U S A* 106:11515-11519.

636 Pelli DG (1997) The VideoToolbox software for visual psychophysics: transforming numbers into movies.
637 *Spat Vis* 10:437-442.

638 Pleskac TJ, Busemeyer JR (2010) Two-stage dynamic signal detection: a theory of choice, decision time,
639 and confidence. *Psychol Rev* 117:864-901.

640 Rahnev D, Denison RN (2018) Suboptimality in Perceptual Decision Making. *Behav Brain Sci*:1-107.

641 Ratcliff R, Smith PL (2004) A comparison of sequential sampling models for two-choice reaction time.
642 *Psychol Rev* 111:333-367.

643 Ratcliff R, McKoon G (2008) The diffusion decision model: theory and data for two-choice decision tasks.
644 *Neural Comput* 20:873-922.

645 Roitman JD, Shadlen MN (2002) Response of neurons in the lateral intraparietal area during a combined
646 visual discrimination reaction time task. *J Neurosci* 22:9475-9489.

647 Shadlen MN, Newsome WT (2001) Neural basis of a perceptual decision in the parietal cortex (area LIP)
648 of the rhesus monkey. *J Neurophysiol* 86:1916-1936.

649 Smith PL, Vickers D (1988) The Accumulator Model of 2-Choice Discrimination. *J Math Psychol* 32:135-
650 168.

651 Swets J, Tanner WP, Jr., Birdsall TG (1961) Decision processes in perception. *Psychol Rev* 68:301-340.

- 652 Treue S, Hol K, Rauber HJ (2000) Seeing multiple directions of motion-physiology and psychophysics. Nat
653 Neurosci 3:270-276.
- 654 Vickers D (1979) Decision Processes in Visual Perception: Academic Press.
- 655 Wright DB, Varley S, Belton A (1996) Accurate second guesses in misinformation studies. Appl Cognitive
656 Psych 10:13-21.
- 657 Zylberberg A, Barttfeld P, Sigman M (2012) The construction of confidence in a perceptual decision.
658 Front Integr Neurosci 6:79.
- 659

660 **Table 1. List of motion coherence combinations**

Motion coherence of first component [%]	Motion coherence of second component [%]	Motion coherence of third component [%]
0	0	0
5	0	0
0	5	0
0	0	5
10	0	0
0	10	0
0	0	10
20	0	0
0	20	0
0	0	20
40	0	0
0	40	0
0	0	40
10	10	10
20	10	10
10	20	10
10	10	20
30	10	10
10	30	10
10	10	30

20	15	5
20	5	15
15	20	5
5	20	15
15	5	20
5	15	20
30	15	5
30	5	15
15	30	5
5	30	15
15	5	30
5	15	30
20	20	20
30	20	20
20	30	20
20	20	30
40	20	20
20	40	20
20	20	40
30	25	15
30	15	25
25	30	15
15	30	25

25	15	30
15	25	30
40	25	15
40	15	25
25	40	15
15	40	25
25	15	40
15	25	40

661

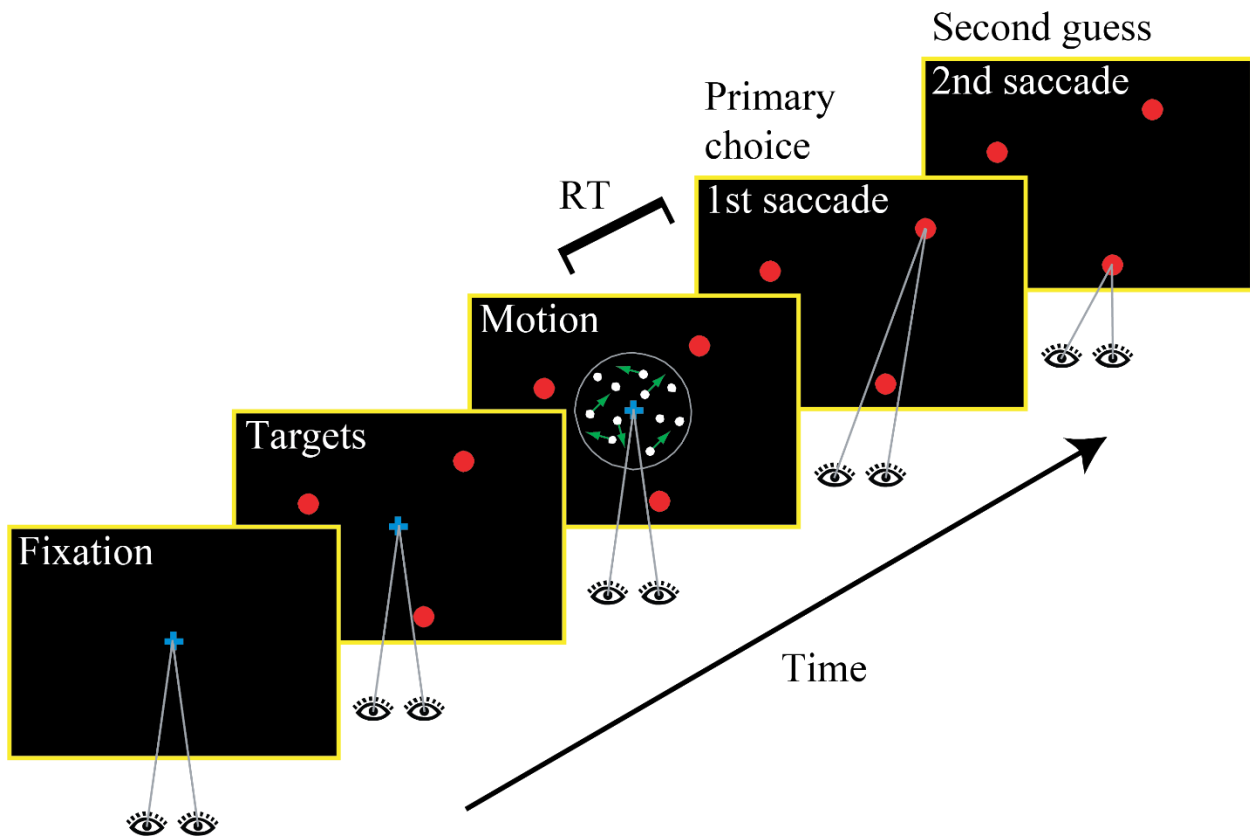
662

663 **Table 2. Best-fitting model parameters**

Model parameters	Parameter values
g	0.0103
k_n	0.197
k_s	0.616
k_v	0.329
Residual time (ms)	663

664

665

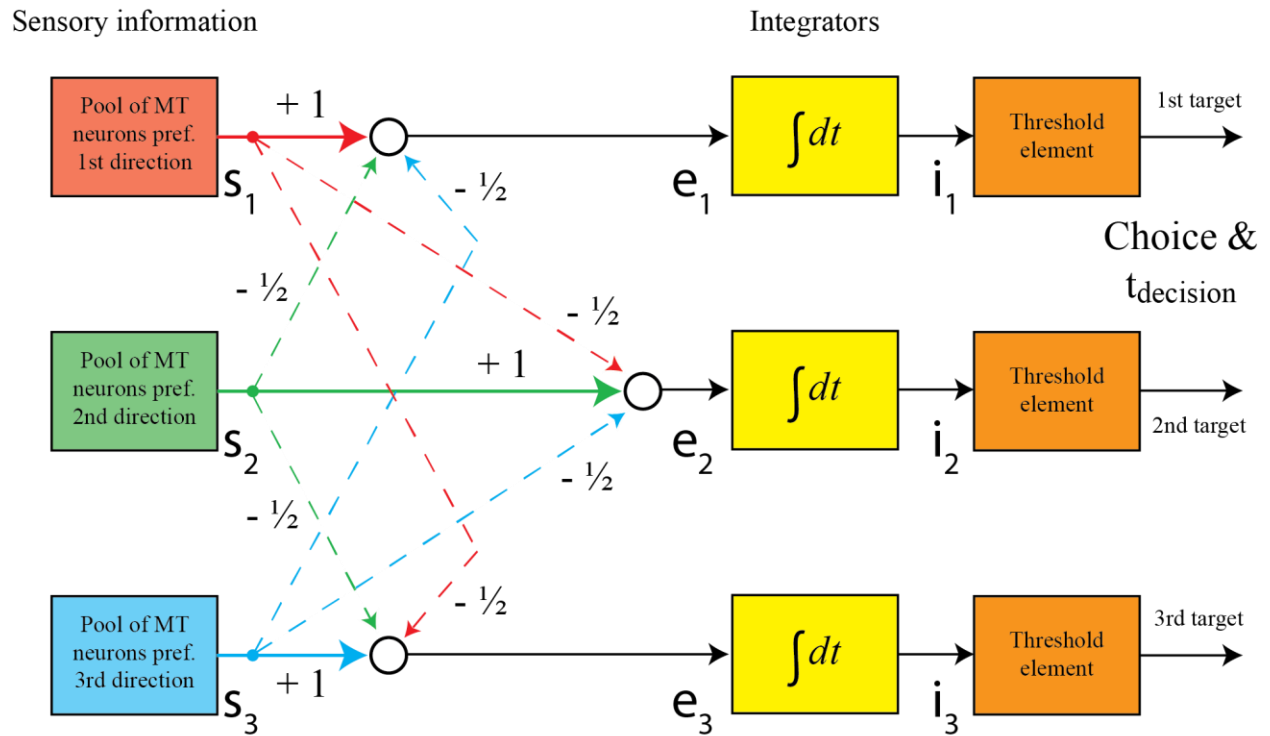


666

667

668 **Figure 1.** Experimental paradigm. Human subjects were asked to determine the strongest motion
 669 direction in a random-dot pattern with multiple motion components. They were free to watch the
 670 stimulus as long as they wanted and responded with a goal-directed eye movement to one of three
 671 choice targets to indicate their primary choice. Choices and RTs were measured. After indicating their
 672 primary choice, subjects were instructed to make a second goal-directed eye movement to one of the
 673 remaining two targets to indicate a second guess.

674

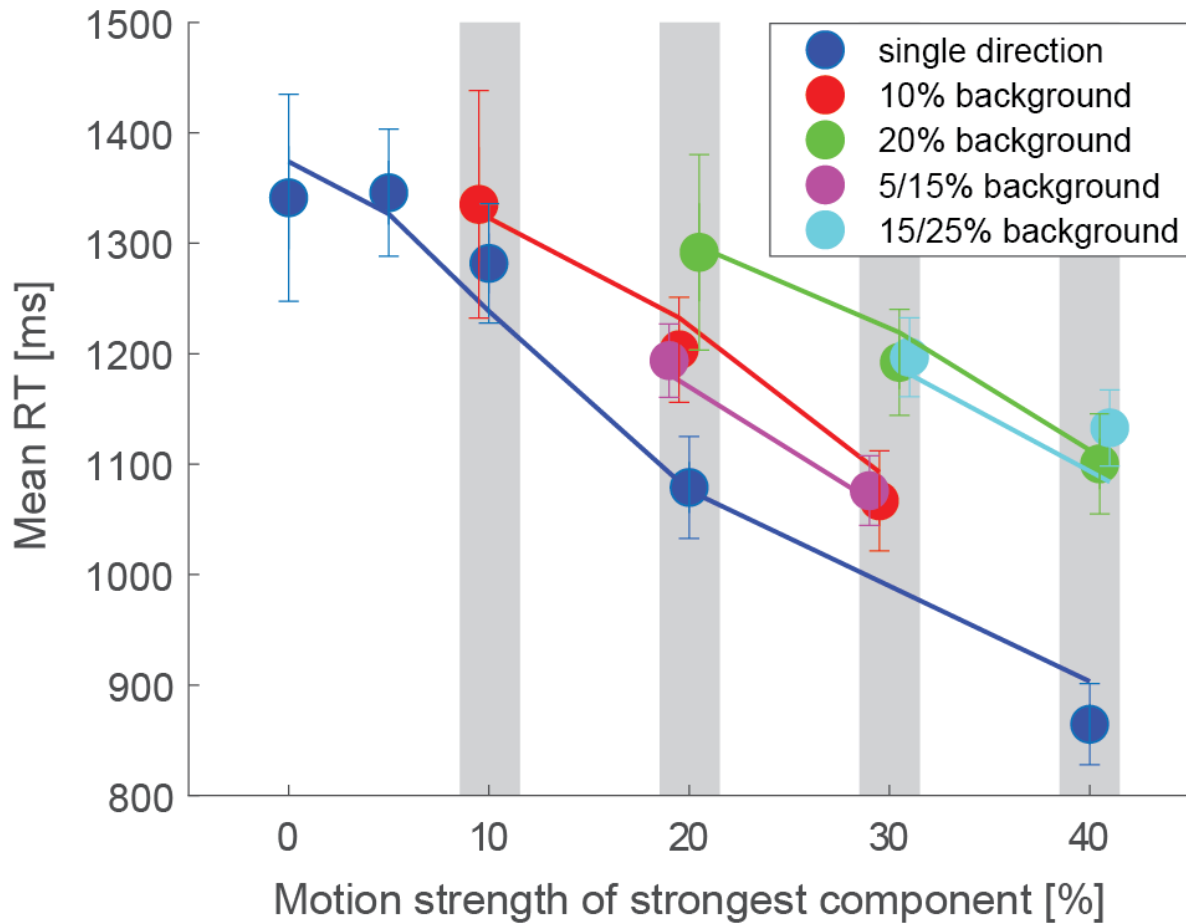


675

676

677 **Figure 2.** Computational model. Three integrators (each associated with one of the three alternatives)
 678 race against each other. The integrator output signal (i_1 , i_2 , or i_3) reaching a decision threshold first
 679 determines the primary choice and terminates the decision process. The integrator input signals (e_1 , e_2 ,
 680 and e_3) are net evidence signals, which are linear combinations of the three relevant sensory signals
 681 (s_1 , s_2 , and s_3). Solid arrows indicate positive weights (excitatory connections), and dashed arrows
 682 indicate negative weights (inhibitory connections). The second guess is determined by the rank ordering
 683 of the remaining two integrators when the winning one reaches threshold.

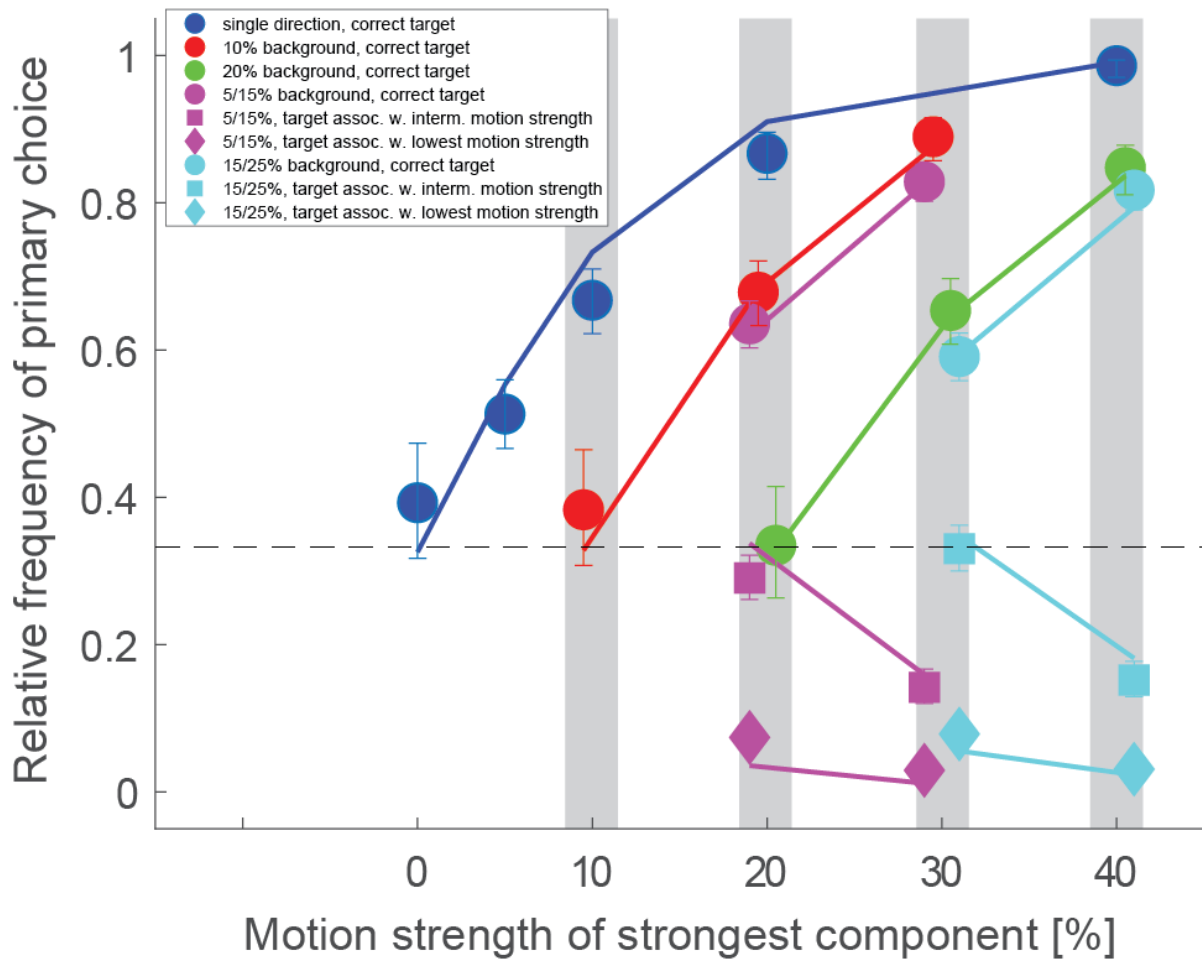
684



685

686

687 **Figure 3.** Mean response time data and fitted model. The symbols represent the measured mean RTs for
 688 all unique combinations of motion strengths. The motion strength of the strongest component is plotted
 689 on the horizontal axis. Colors indicate the motion strengths of the two weaker motion components. (For
 690 example, the cyan point at 40% motion strength indicates the mean RT for stimuli with the three motion
 691 components having strengths of 40%, 25%, and 15%, respectively.) Some points have been shifted
 692 slightly horizontally to reduce graphical overlap. For example, all points within the gray bar centered on
 693 20% have a strength of the strongest motion component of exactly 20%. Error bars indicate 95%
 694 confidence intervals. The lines connect the mean RTs from the computational model.



695

696

697 **Figure 4.** Comparison between the relative frequencies of primary choices and model predictions.

698 Symbols again reflect the data, with error bars indicating 95% confidence intervals. The lines connect

699 the relative frequencies predicted by the computational model. Circles indicate choices of the target

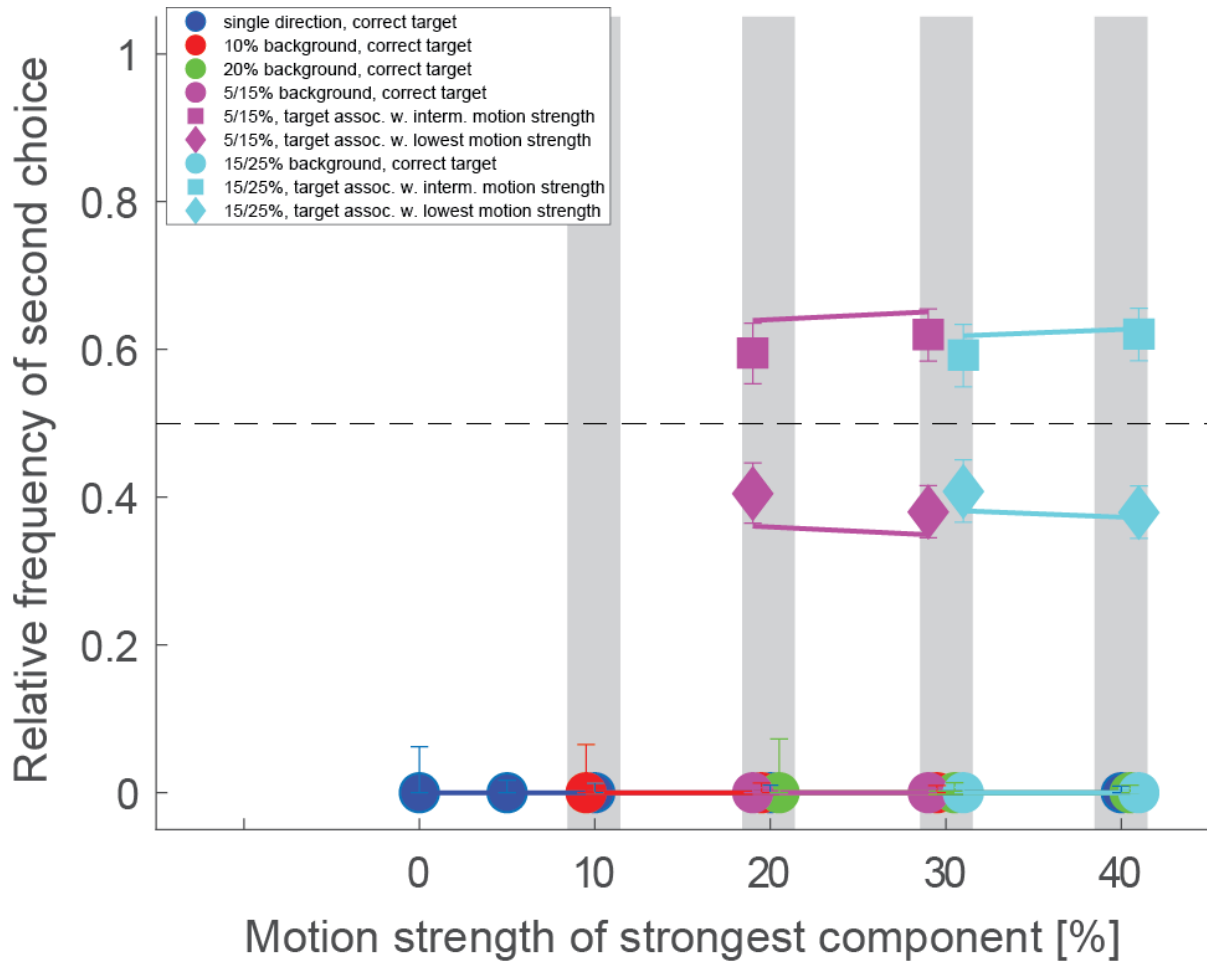
700 associated with the strongest motion component (correct primary choices), squares choosing the target

701 associated with the component with intermediate motion strength, and diamonds choosing the target

702 associated with the weakest motion component. Other conventions as in Fig. 3. The dashed line

703 indicates chance performance.

704



705

706

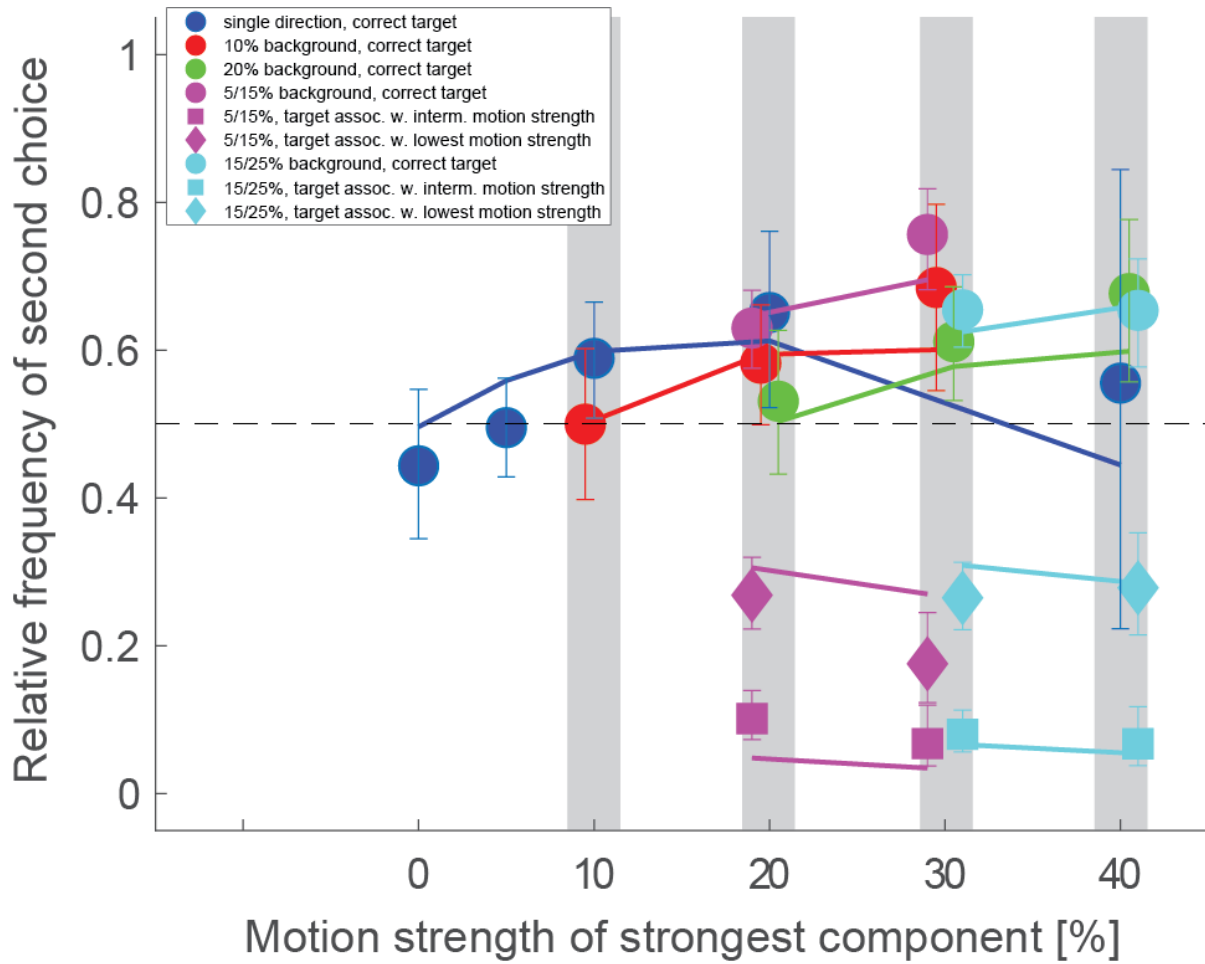
707 **Figure 5.** Comparison between relative frequencies of second guesses on correct trials (symbols, with
 708 error bars indicating 95% confidence intervals) and model predictions (lines). Conventions as in Fig. 4.

709 Note that on correct trials the target associated with the strongest motion component has been

710 reported as the primary choice and is not available for the second guess. Therefore, all circles are

711 located at a relative frequency of zero.

712



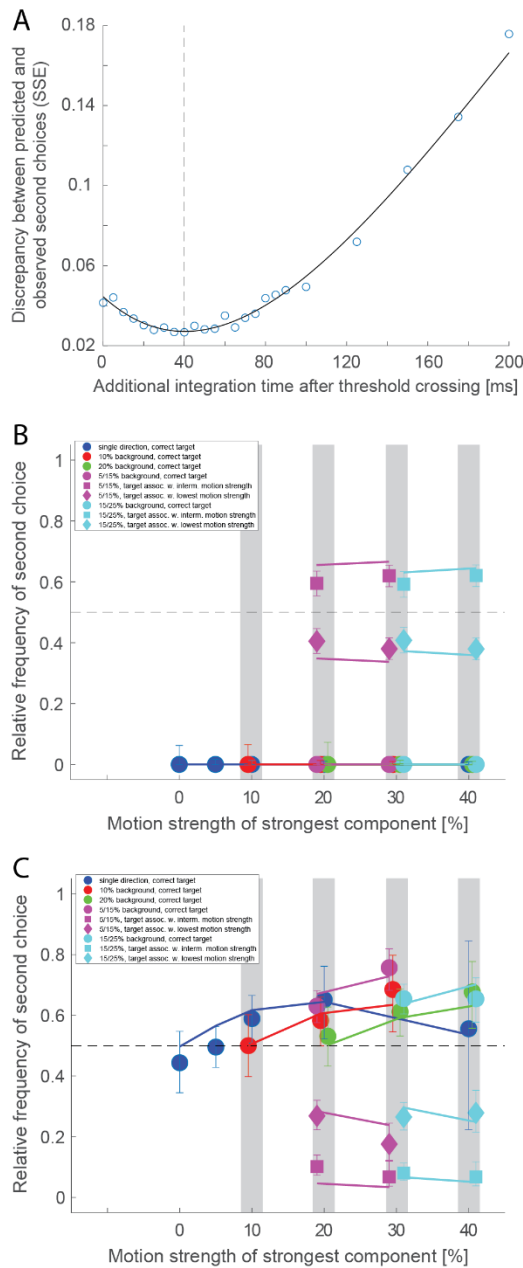
713

714

715 **Figure 6.** Comparison between relative frequencies of second guesses on error trials (symbols, with
 716 error bars indicating 95% confidence intervals) and model predictions (lines). Conventions as in Fig. 5.

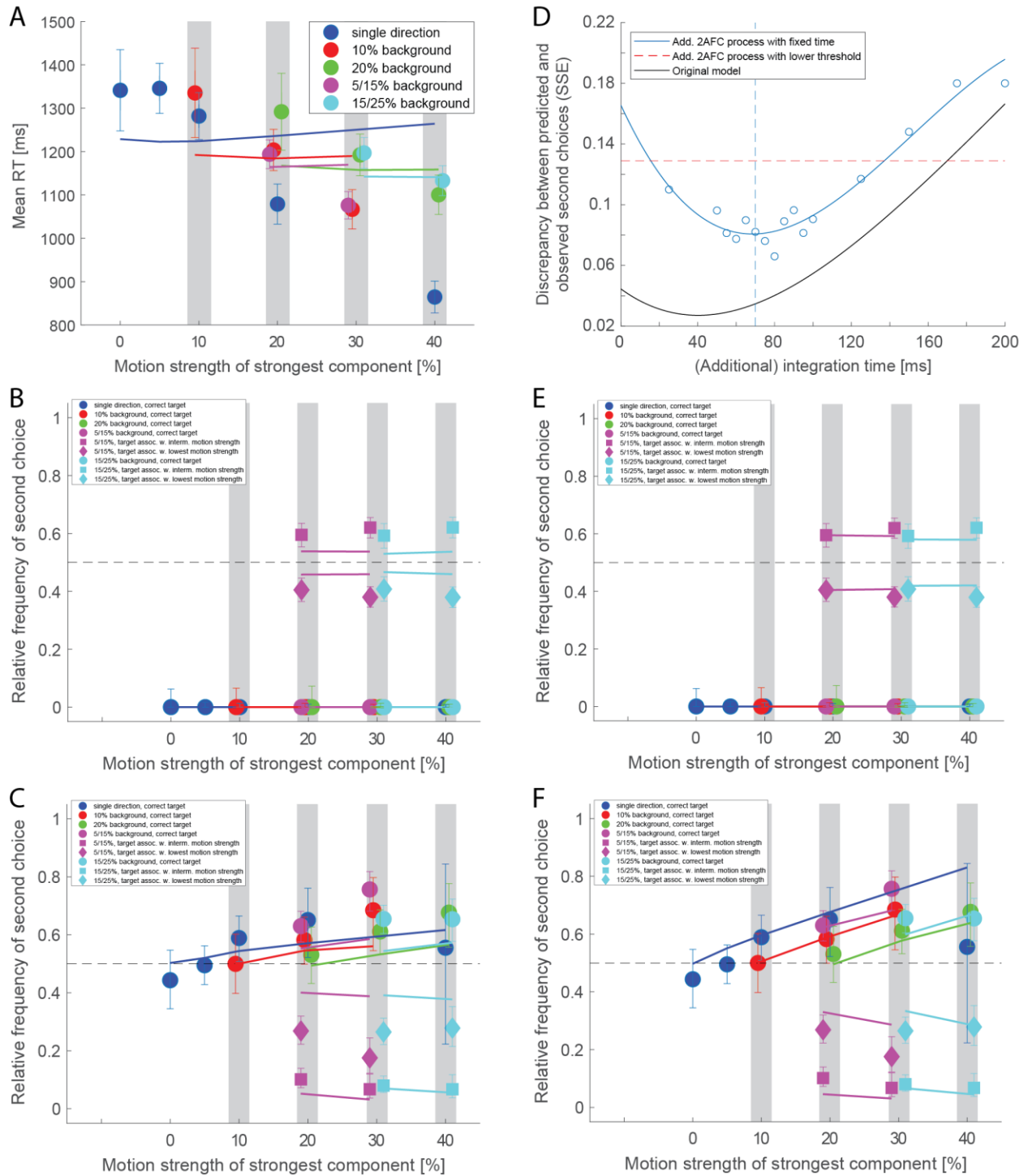
717 How often the correct target (circles) was reported as the second choice varied across experimental
 718 conditions, but was overall significantly above chance (63%).

719



720

721 **Figure 7.** Predictions for second guesses when integration is allowed to continue after the threshold
 722 crossing. **A.** Discrepancy between predicted and observed second guesses as a function of additional
 723 integration time before the accumulated evidence is read out. A minimum (best match) is observed at
 724 40 ms. **B.** Predicted second guesses on correct trials with 40 ms additional integration time (same format
 725 as Fig. 5). **C.** Predicted second guesses on error trials with 40 ms additional integration time (same
 726 format as Fig. 6).



727

728 **Figure 8.** Alternative models. **A.** Mean RT fit for a model that waits for a second threshold crossing, but

729 allowing leaky integration and collapsing bounds (same format as Fig. 3). **B.** Predicted second guesses on

730 correct trials for a model that starts a new 2AFC decision process to determine the second choice and

731 waits for a threshold crossing, but allowing a lower threshold than in the primary decision process (same
732 format as Fig. 5). **C.** Like B, but for error trials (same format as Fig. 6). **D.** Discrepancy between predicted
733 and observed second guesses as a function of integration time for a model that starts a new 2AFC
734 decision process to determine the second choice and reads the process out after a fixed amount of time
735 (blue). A minimum (best match) is observed at 70 ms. For comparison, the curve for the original model
736 (black) and the value for the model with a low threshold (red) are also shown. **E.** Predicted second
737 guesses on correct trials for a model that starts a new 2AFC decision process to determine the second
738 choice and integrates the sensory evidence for 70 ms before the process is read out (same format as
739 Fig. 5). **F.** Like E, but for error trials (same format as Fig. 6).

740